

INVESTIGATION INTO A TRACE EFFECT OF THE SPACE SHUTTLE LAUNCH ON THE OPTICAL CHARACTERISTICS, OZONE, AND AEROSOL OF THE UPPER ATMOSPHERE BY THE METHOD OF TANGENT SENSING FROM A BOARD OF THE ASTROPHYSICAL SPACE STATION ASTRON IN THE ULTRAVIOLET REGION

A.A. Cheremisin, L.V. Granitskii, V.N. Myasnikov, and N.V. Vetchinkin

*Scientific-Research Physical-Technical Institute at the Krasnoyarsk State University
Krasnoyarsk State University*

E.K. Fedorov Institute of Applied Geophysics, Moscow

Received August 4, 1997

Results of investigations of the upper atmosphere by the method of tangent sensing in the ultraviolet region ($\lambda = 280$ nm, $\Delta\lambda = 3$ nm) are presented obtained using an ultraviolet telescope of the Astrophysical Space Station Astron. Vertical profiles of the spectral brightness of the Earth's atmospheric limb have been obtained for points along the active trajectory of the Space Shuttle launch from Cape Canaveral on April 6, 1984. Vertical profiles of spectral brightness of the atmospheric limb obtained before the launch are typical of the unperturbed atmosphere. It is established that after the spacecraft launch a bright scattering aerosol layer is formed at altitudes near 100 km. Its lifetime measured from the launch exceeds 2 h 20 min. Its extension in the direction transverse to the launch trajectory exceeds 900 km. The evidence is given that the thickness of this artificial aerosol layer is only several kilometers, which is typical of noctilucent clouds. No significant influence is found of the spacecraft launch on the aerosol scattering characteristics at altitudes 65–85 km and on the ozone concentration between 55 and 65 km (the characteristic scale of horizontal averaging in tangent sensing is about 10^3 km).

Running engines of launched high-power rocket carriers release combustion products and in some cases even unburnt propellant components into the atmosphere. The resulting aerosol-gaseous trace can be seen by the naked eye from the Earth's surface.¹ Optical effects that can be classified as anomalous are also observed.^{1,2} Character and scale of atmospheric distortions depend on the altitude and regime of a rocket flight. The scale of distortions increases with the altitude. Investigation of these distortions is of importance not only for the study of various atmospheric processes, but also from the ecological viewpoint.³

At altitudes above 100 km, the effects related with the interaction of gaseous combustion products of rocket engines with the ionospheric plasma have attracted the major attention.^{4–6} Meanwhile the influence of the combustion products on the state of ozone and aerosol layers of the upper atmosphere is less well understood.

At high altitudes, artificial aerosol formations are observed during operation of the engines of space vehicles. They have conical shape caused by the

dynamics of combustion product discharge from the engines. Spread of these formations occur with no change of their shape and without stagnation as is the case, for example, for running starting units at an altitude of 20 000 km (see Ref. 7) and for the Rocketdyne J-2 engine of the Saturn-IV V rocket at an altitude of 175 km (see Ref. 8). According to the data of numerous observations, at altitudes above 100 km the artificial formations of the rocket-induced aerosol with characteristic sizes from several tens to several hundreds of kilometers are no longer seen by the naked eye in 10–15 min after their formation.¹

The results of ground-based photographic observations of the stagnation of artificial formation comprising the rocket-induced aerosol in the upper atmosphere released after the launch of the Molniya satellite with the Soyuz rocket were presented in Ref. 7. In accordance with these results, the complete stagnation of the rocket-induced aerosol particles occurs at an altitude of ~100 km. In addition, in Ref. 7 the results were presented of scanning across the active trajectory of the Space Shuttle launch on February 3, 1984 obtained using an ultraviolet telescope of the

Astrophysical Space Station (ASS) Astron at $\lambda = 273$ nm from an altitude of 40 000 km. According to these results, the significant increase of the UV radiation in comparison with its background value is recorded from the region which extends up to 1 000 km in the direction transverse to the launch trajectory 3–4 hours after the Space Shuttle launch. However, the interpretation of the obtained results is complicated by a strong effect of the light scattered in a spectrometer linked with the UV telescope of the ASS Astron for this scheme and conditions of observations. The level of the scattered light under these conditions, according to estimates of Cheremisin et al.,⁹ is nearly twice as large as the useful signal level at $\lambda = 273$ nm. In this case, the scattered light level reaches its maximum at $\lambda = 350$ nm, and even inhomogeneities in the albedo of the Earth's underlying surface and clouds can be recorded.

In the present paper, the results of investigation into a trace effect of the Space Shuttle launch on the parameters of the upper atmosphere by the method of tangent sensing in the ultraviolet region are presented. The experiments were carried out using a UV telescope of the ASS Astron on April 6, 1984, when the Space Shuttle was launched (at 16:58, DST). The ASS Astron was put into the satellite orbit with a perigee of 200 000 km, an apogee of 2 000 km, an angle of orbit inclination of 56°, and a rotation period of 96 h. First, the entire ASS was turned to sight the optical axis of the telescope on the given point of the Earth's surface. Then the optical axis of the telescope moved along the Earth's surface toward its edge and intersected the atmospheric limb as the ASS orbited while its orientation in relation to stars remained unchanged. In the given experiment, the distance from the ASS to the tangential points was about 180 000 km. A 12" offset diaphragm was used as a working diaphragm of the spectrometer. The halfwidth of the instrumental function (vertical range of data averaging) was about 8 km. The telescope allowed for scans at a wavelength of 280 nm with spectral resolution of 3 nm. Readings were taken in 0.61 s with altitude step varying from 0.6 to 1.5 km for individual scans.

Procedures for data processing, altitude referencing of the experimental curves of spectral brightness, absolute calibration of brightness, considering the contribution from the light scattered in the spectrometer, calculating the spectral brightness, and solving inverse problems were described in Ref. 9, where they were refined and used to investigate the background unperturbed state of the atmosphere. It is important that the level of the useful signal exceeded by an order of magnitude the level of light scattered in the spectrometer in case of tangent sensing when the brightness of the Earth's atmospheric limb was measured. In addition, the employed procedure for data processing allowed the contribution of the scattered light to be estimated fairly exactly from synchronous readings of a photomultiplier in the second

UV channel and corresponding corrections to be introduced.

Fig. 1 shows positions of the tangential points on the active trajectory of Space Shuttle launch on April 6, 1984. The trajectory of Space Shuttle launch on February 3, 1984, was typical. A typical running time of the SSME liquid-propellant rocket engine in flight is 520 s and the length of the active trajectory is 1 800 km. Errors in altitude referencing due to errors in telescope sighting on the point of aim after ASS turning and stabilization errors are also shown in Fig. 1. For each point, the major semiaxis of the error ellipse was 100 km long and the minor semiaxis was 20 km long. The line of sight to the tangential point intersected the active trajectory of Space Shuttle launch at an angle of 60° and had nearly meridian direction, that is, scanning was performed across the active trajectory. Scattering angles varied from 94 to 96.4° for different scans. Solar zenith angles at the tangential points changed from 59.8° for scan 1 to 24.6° for scan 7.

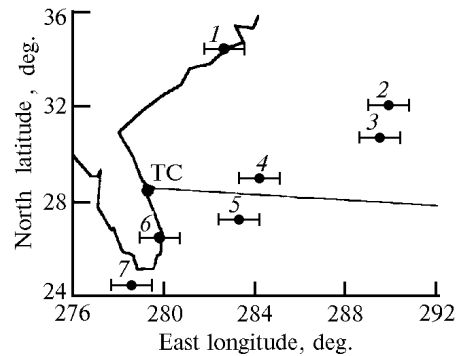


FIG. 1. Positions of the tangential points on the active trajectory of the Space Shuttle launch on April 6, 1984, in case of remote sensing of the atmosphere from a board of the Astrophysical Space Station Astron in the ultraviolet region. The time period before the launch: 1) 37 min, 2) 11 min. The time period after the launch: 3) 15 min, 4) 1 h 5 min, 5) 1 h 30 min, 6) 1 h 54 min, 7) 2 h 20 min.

By scanning the atmospheric limb of the Earth, the corresponding vertical profile of the spectral brightness of the atmosphere was obtained at $\lambda = 280$ nm. Some fragments of experimental dependences are shown in Fig. 2 in the form of dependences $I_{a\lambda} = I_{\lambda} - I_{R\lambda}$ on the altitude, where I_{λ} is the experimentally measured spectral brightness of the atmosphere and $I_{R\lambda}$ is the spectral brightness of pure Rayleigh molecular scattering. It was calculated in the same way as in Ref. 9 in the single scattering approximation for atmospheric models that consider seasonal-latitudinal and diurnal variations of the atmospheric density. The numbers adjacent to the curves here and in the following figures denote the

serial numbers of the tangential points in Fig. 1. These experimental dependences were smoothed with the Gauss point filter. The significant excess of the experimental brightness I_λ over the level of pure molecular scattering at altitudes 65–110 km can be related with the effect of aerosol scattering.

Curves 1 and 2 in Fig. 2 were obtained before the Space Shuttle launch. They characterize the background state of the atmosphere. Curve 2 is typical (average) for the unperturbed background state of the atmosphere.⁹

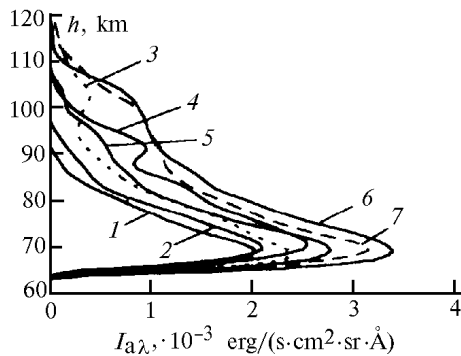


FIG. 2. Vertical profiles of the spectral brightness of the atmosphere $I_{a\lambda}$ caused by aerosol scattering from the data of observations from a board of the Astrophysical Space Station Astron along the active trajectory of the Space Shuttle launch.

As can be seen from Fig. 2, curves 3–7 obtained after the Space Shuttle launch, in contrast with curves 1–2, have the maxima of aerosol scattering between 92 and 103 km. These maxima of aerosol scattering can be considered as a result of the Space Shuttle launch. In this case, from 15 min to 2 h 20 min after the launch, there was no clearly pronounced tendency for a decrease of the intensity of these maxima; therefore we believe that the perturbed state of the upper atmosphere persists many hours after the launch. The recorded brightness of these scattering maxima was about $1 \cdot 10^{-3} \text{ erg}/(\text{s}\cdot\text{cm}^2\cdot\text{sr}\cdot\text{\AA})$ for $\lambda = 280 \text{ nm}$, which is about 5% of the maximum brightness of the atmospheric limb at $h = 58 \text{ km}$. Tangential point 3 (see Fig. 1) was at a distance of about 320 km from the active launch trajectory and tangential point 7 – at about 460 km; therefore, the transverse size of the perturbed zone in this case exceeded 900 km. Thus, after the Space Shuttle launch fairly bright aerosol scattering layer was formed near 100 km.

Figure 3 shows the curves that characterize variations of the spectral brightness of the atmosphere between 85 and 110 km due to the trace effect of the Space Shuttle launch. The variations of the spectral brightness were estimated for curves 3, 4, and 6 with the most clearly pronounced maxima of aerosol scattering near 100 km. The solid lines show the instrumental functions of the telescope of the ASS

Astron after corresponding scaling. The instrumental function is the effective point spread function which characterizes the radiation flux produced by a point source which is incident on the spectrometer through the 12" input diaphragm as a function of the point source coordinates. It was calculated by solving the inverse problems from the data of specially organized outdoor observations of the Earth and Moon disks illuminated with the Sun. Here, the instrumental function was transformed into the line spread function. The normalization condition for this function and its position were specially selected for curves 3, 4, and 6 so that the maximum of the instrumental function coincided with the maximum of the excess brightness. As can be seen, curves 3, 4, and 6 practically coincide with the instrumental function. This is the case for the radiation source whose width is less than the width of the instrumental function. Hence, there are grounds to believe that the observed aerosol formation has a thickness of several kilometers typical of noctilucent clouds most often observed at lower altitudes between 80 and 83 km.

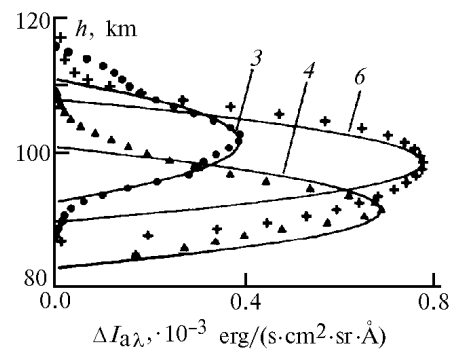


FIG. 3. Estimated variations of the spectral brightness of the atmosphere $\Delta I_{a\lambda}$ between 85 and 110 km due to the trace effect of the Space Shuttle launch. For comparison, the solid lines show the instrumental function of the telescope after corresponding scaling.

The vertical profiles of the average volume coefficient of the differential aerosol light scattering and of the turbidity coefficient were reconstructed from the vertical profiles of the spectral brightness of the atmosphere obtained after the Space Shuttle launch (see Fig. 2) and under conditions of the background unperturbed state of the atmosphere. Within the anthropogenic layer between 85–110 km, the maximum values of the turbidity coefficient for different curves were between 15 and 60. However, at altitudes from 80–85 km to 65 km we did not establish any significant change of the aerosol scattering pattern which was within the limits of permissible variations. Thus, the trace effect of the Space Shuttle launch on the parameters of aerosol scattering and the spectral brightness was not observed at altitudes from 65 to 80–85 km in case of tangent sensing of the atmosphere.

Here, it should be mentioned that at lower altitudes the brightness of the atmospheric limb increased and the scale of horizontal averaging was about 10^3 km in case of tangent sensing.

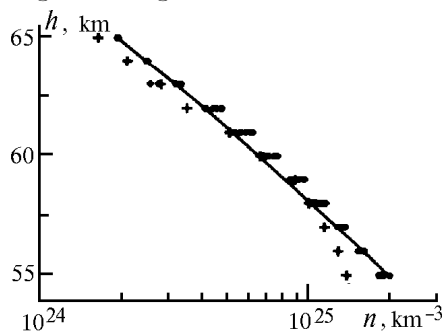


FIG. 4. Vertical profiles of the ozone concentration reconstructed from the data of observations from a board of the ASS Astron for points along the active trajectory of the Space Shuttle launch on April 6, 1984 (●). Solid line is for the model profile borrowed from Ref. 13; +, from the data of Ref. 14.

Figure 4 shows the results of reconstruction of the vertical profiles of the ozone concentration at altitudes between 55 and 65 km from the vertical profiles of the spectral brightness of the Earth's atmospheric limb. In the process of reconstruction, the aerosol layer between 65 and 110 km was taken into account. Our calculations have shown that the reconstructed values of the ozone concentration between 55 and 63 km will change only by 1–2% if we ignore the effect of the aerosol layer. So in this case we neglect the aerosol scattering. This can be justified as in Ref. 9. First, according to the model for the optical characteristics suggested in Ref. 10, which is in good agreement with rocket data presented in Ref. 11, the aerosol scattering at these altitudes is relatively small in comparison with the molecular scattering. It is 3–6% of the molecular scattering. Second, the effect of the aerosol scattering is masked by the error in measuring the vertical profiles of the spectral brightness of the atmosphere.

Good agreement can be seen of the ozone profiles obtained under conditions of the background unperturbed state of the atmosphere (the profiles reconstructed from the data of scans 1 and 2 of the present paper and the profiles presented in Refs. 9 and 12) and the ozone profiles obtained after the Space Shuttle launch as well as the model data borrowed from Ref. 13. The observed deviation from the model dependence is somewhat greater than the standard deviation, which for this latitude and season is $\pm 4\%$ for $h = 55$ km according to model described in Ref. 13. On the one hand, the deviation of the obtained profiles of the ozone concentration from the model profiles may be due to the error in measuring the brightness. However, on the other hand, the profile of the ozone concentration obtained with the help of a rocket optical ozonesonde from the data of measuring the attenuation

of the directly transmitted solar radiation at $\lambda = 255$ nm and a solar zenith angle of 90° (see Ref. 14), shown in Fig. 4 for comparison, also differs noticeably from the corresponding model profile. The ozone profiles obtained after the Space Shuttle launch do not differ from the background ozone profiles. Thus, taking into account the horizontal scale of averaging being equal to about 10^3 km, we can conclude that for time periods from 15 min to 2 h 20 min we have not reveal any significant effect of the Space Shuttle launch on the ozone layer between 55 and 65 km.

As to the origin of the long-lived anthropogenic aerosol layer between 90–100 km, we consider two possible mechanisms of its formation. First, the layer comprises the dispersed particles formed when the combustion products (water vapor) in flames from jet engines of space vehicles expand and then decelerate near 100 km. This is confirmed by the data of ground-based observations of the launch of the rocket carrier Soyuz⁷ that the complete stagnation of the aerosol formation occurs near 90–100 km. The average radius of the particles of these aerosol formations r can be estimated by solving the system of kinetic equations for micrometeoroid bodies.^{15,16}

The formula relating the velocity of particle v with the altitude h can be easily derived through integration of the stagnation equation (with the quadratic dependence of the stagnation force on the velocity)

$$\ln \left(\frac{v_\infty}{v} \right) = \frac{3}{4} \frac{\Gamma \Delta H \rho_a(h)}{\cos Z_R \rho_{\text{pat}} r}.$$

Here, v_∞ is the initial particle velocity, $\cos Z_R$ is the cosine of the zenith angle for the meteor radiant of the particle, and ρ_{pat} is the density of the material of the particle. In the derivation of this formula, we ignored the effect of ablation due to small initial velocities of particles in comparison with those of micrometeoroid bodies and the effect of gravitational forces. The particles were considered spherical and the exponential dependence of the atmospheric density on the altitude $\rho_a(h) \sim \exp(-h/\Delta H)$ was assumed, where ΔH is the height of the homogeneous atmosphere. Using the following values of the parameters: $\rho_a(h) = 6 \cdot 10^{-7}$ kg/m³ for an altitude of 100 km, $\Delta H = 8$ km, $\Gamma = 1$, $\rho_{\text{pat}} = 10^3$ kg/m³, $\cos Z_R = 1$, $\ln(v_\infty/v) = 6.2$ ($v_\infty \sim 4$ km/s and $v \sim 100$ m/s at an altitude of 100 km is an estimate of the final stagnation velocity when deceleration occurs with the sedimentation rate at this altitude), we obtain $r = 1$ μm and the mass of the particle $m = 4 \cdot 10^{-12}$ g. The further evolution of the aerosol layer comprising stagnated particles and its lifetime depend on many factors. In particular, the rate of sedimentation of particles having the above indicated radius, calculated by the formula given in Refs. 17 and 18, is 100 m/s at an altitude of 100 km, 20 m/s at 90 km, and 3 m/s at 80 km. The lifetime of the layer located between 90 and 100 km that comprises the particles of the above-indicated

radius can be defined as the time of their gravitational settling and is several minutes. The lifetime (the settling time) of particles with smaller radius is increased inversely proportional to their radius and may exceed 3 h for particles with radii smaller than 20 nm.

The other mechanism of formation of the long-lived aerosol layer between 90 and 100 km may be connected with the saturation of the upper atmosphere by water vapor, which is the main gaseous component of the combustion products of space vehicle engines, near the turbopause. In this case, the mechanism of formation of the examined aerosol layer may be similar to the mechanism of formation of noctilucent clouds. According to the condensation model, the noctilucent clouds observed between 80 and 83 km are formed at high latitudes in the cold summer mesosphere supersaturated with water vapor. In this case, as the model calculations of Ref. 18 have shown, large-scale supersaturated regions are formed within the 10-km altitude range, whereas the observed noctilucent clouds have typical thicknesses of the order of several kilometers. Small-scale and mesoscale structures of noctilucent clouds are assumed to be caused by local wave processes in the atmosphere.

Our data allow us to suggest that the thickness of the aerosol layer formed between 90 and 100 km after the Space Shuttle launch is only several kilometers. It is possible that this is a consequence of the common features in mechanisms of the formation of this layer and noctilucent clouds. It is reasonable to suppose that the meteor dust particles or particles formed due to recondensation of meteor vapor serve as condensation nuclei in noctilucent clouds. In this connection, the fact that according to the data of unique radar observations at frequencies 2–6 MHz reported in Ref. 19, the concentration of the meteors has the peak at an altitude of 105 km has engaged our attention (at higher frequencies, for example, at a frequency of 54 MHz, the peak of the concentration is observed at an altitude of 95 km). This altitude is close to the altitude of location of the aerosol layer observed by us after the Space Shuttle launch.

The formation of aerosol layers between 90 and 100 km after the launch of the Space Shuttle or other space vehicles is connected with relatively poorly known complex processes in the upper atmosphere and further investigations of such artificial aerosol formations may help to illuminate the nature and mechanisms of evolution of these processes.

REFERENCES

1. Yu.V. Platov and V.V. Rubtsov, *UFO and Modern Science* (Nauka, Moscow, 1991), 176 pp.
2. V.N. Novosel'tsev, *Izv. Akad. Nauk SSSR, Fiz. Atmos. Okeana* **26**, No. 6, 614–621 (1990).
3. L.S. Nesterov, N.N. Petrov, and Yu.A. Romanovskii, *Ecological Aspects of Cosmonautics* (Znanie, Moscow, 1986), 64 pp.
4. M. Mendillo, *Adv. Space Res.* **2**, No. 3, 150–159 (1982).
5. P.A. Bernhardt, *Adv. Space Res.* **2**, No. 3, 129–149, (1982).
6. V.D. Karlov, S.I. Kozlov, and G.N. Tkachev, *Kosm. Issled.* **18**, No. 2, 266 (1980).
7. N.V. Vetchinkin, L.V. Granitskii, Yu.V. Platov, and A.I. Sheikhet, *Kosm. Issled.* **31**, No. 1, 93–100, (1993).
8. R.T.V. Kung, L. Cianciolo, and J.A. Myer, *Rock. Engin.*, No. 4, 21–29 (1975).
9. A.A. Cheremisin, L.V. Granitskii, V.N. Myasnikov, et. al., *Atmos. Oceanic Opt.* **10**, No. 12, 885–890 (1997).
10. G.M. Krekov and S.G. Zvenigorodskii, *Optical Model of the Middle Atmosphere* (Nauka, Novosibirsk, 1990), 278 pp.
11. A.E. Mikirov and V.A. Smerkalov, *Investigation of the Scattered Radiation in the Upper Earth's Atmosphere* (Gidrometeoizdat, Leningrad, 1981), 208 pp.
12. L.V. Granitskii and A.A. Cheremisin, in: *Abstracts of Reports at the All-Union Conference on Atmospheric Ozone, Suzdal'* (1988), p. 63.
13. G.M. Keating, D.T. Young, and M.C. Pitts, *Adv. Space Res.* **7**, No. 10, (10)105–(10)115 (1987).
14. T. Watanabe and T. Ogawa, *Adv. Space Res.* **7**, No. 9, (9)123–(9)126 (1987).
15. V.A. Bronshten, *Physics of Meteoric Phenomenon* (Nauka, Moscow, 1981), 416 pp.
16. P. Pecina, *Bull. Astron. Inst. Czechosl.* **40**, No. 6, 367–378 (1989).
17. R.P. Turco, O.B. Toon, P. Hamill, et al. *J. Geophys. Res.* **86**, No. C2, 1113–1128 (1981).
18. M. Memmesheimer and P.W. Blum, *Physica Scripta* **37**, 178–184 (1988).
19. D. Olsson-Steel and W.G. Elford, *Publ. Astron. Inst. Czechosl. Acad. Sci.*, No. 67, 193–197 (1987).